

Journal of Materials Chemistry C

Accepted Manuscript



This is an *Accepted Manuscript*, which has been through the Royal Society of Chemistry peer review process and has been accepted for publication.

Accepted Manuscripts are published online shortly after acceptance, before technical editing, formatting and proof reading. Using this free service, authors can make their results available to the community, in citable form, before we publish the edited article. We will replace this *Accepted Manuscript* with the edited and formatted *Advance Article* as soon as it is available.

You can find more information about *Accepted Manuscripts* in the [Information for Authors](#).

Please note that technical editing may introduce minor changes to the text and/or graphics, which may alter content. The journal's standard [Terms & Conditions](#) and the [Ethical guidelines](#) still apply. In no event shall the Royal Society of Chemistry be held responsible for any errors or omissions in this *Accepted Manuscript* or any consequences arising from the use of any information it contains.

Cite this: DOI: 10.1039/c0xx00000x

www.rsc.org/xxxxxx

Mechano-induced Luminescent and Chiroptical Switching in Chiral Cyclometalated Platinum(II) Complexes

Xiao-Peng Zhang, Jin-Feng Mei, Jian-Cheng Lai, Cheng-Hui Li,* Xiao-Zeng You*

Received (in XXX, XXX) Xth XXXXXXXXX 20XX, Accepted Xth XXXXXXXXX 20XX

DOI: 10.1039/b000000x

A couple of enantiomeric chiral cyclometalated platinum(II) complexes [Pt((-)-L₁)(Dmp_i)]Cl ((-)-**1**) and [Pt((+)-L₁)(Dmp_i)]Cl ((+)-**1**) [(-)-L₁ = (-)-4,5-pinene-6'-phenyl-2,2'-bipyridine, (+)-L₁ = (+)-4,5-pinene-6'-phenyl-2,2'-bipyridine, Dmp_i = 2,6-dimethylphenylisocyanide] were synthesized. Two polymorphs (**Form-Y** and **Form-R**) of complex (-)-**1** have been obtained. The crystallographic studies of both forms revealed that the emission and electronic circular dichroism (ECD) spectra of these complexes at solid state were sensitive to intermolecular effects and molecular surrounding environments. The yellow forms (**Form-Y**) of complexes (-)-**1** and (+)-**1** were found to undergo crystal-to-amorphous transformation upon mechanical grinding, resulting in luminescent and chiroptical switching behaviours as evidenced by emission and ECD spectra. The mechanochromic process can be reversed repeatedly by addition a few drops of dichloromethane. When the counteranions Cl⁻ in **1** was replaced by trifluoromethanesulfonate (OTf⁻), complexes [Pt((-)-L₁)(Dmp_i)]OTf ((-)-**2**) and [Pt((+)-L₁)(Dmp_i)]OTf ((+)-**2**) were obtained. Complexes (-)-**2** and (+)-**2** showed a more pronounced luminescent switching behaviour, suggesting that the switching properties can be tuned by counteranions.

Introduction

Chiroptical molecular switches or sensors have attracted intense attentions due to their extensive applications in high-technology fields, such as chiroptical sensing, optical displays, and information storage.¹ In most cases, the chiroptical switching behaviours were originated from changes of molecular conformations or intermolecular arrangements upon changing the temperature and solvent polarity, adding acid-base, metal ions, counter anions, or reducing/oxidizing agents, or applying external stimuli such as electrochemical potential, and light irradiation, and so on.²

Benefited from environmentally sensitive metal-metal interactions and π-π contacts, square-planar platinum(II) complexes were found to form dimer or oligomer upon external stimuli (solvent, organic vapor, mechanical force, temperature, etc.),³⁻⁷ consequently leading to interesting stimuli-responsive phenomena (solvatochromism, vapochromism, mechanochromism and thermochromism).⁸ For some platinum(II) complexes with functional ligands, dual-stimulus-responsive or multi-stimulus-responsive switching behaviours were observed.^{6b,7b,8d} To date, most of stimuli-responsive systems containing platinum(II) complexes are characterized by changes of absorption and/or emission, an alternation of chiroptical properties upon external stimuli (ie. chiroptical sensors) is sparse.⁹

We have previously studied the vapor-induced chiroptical

switching phenomenon of chiral cyclometalated platinum(II) complexes^{9e} and the helical aggregation behaviours of aqueous solution of an couple of enantiomeric cyclometalated platinum(II) complexes [Pt((-)-L₁)(Dmp_i)]Cl ((-)-**1**) and [Pt((+)-L₁)(Dmp_i)]Cl ((+)-**1**) [(-)-L₁ = (-)-4,5-pinene-6'-phenyl-2,2'-bipyridine, (+)-L₁ = (+)-4,5-pinene-6'-phenyl-2,2'-bipyridine, Dmp_i = 2,6-dimethylphenylisocyanide] (Fig. 1).¹⁰ As the extension of our previous works, we found that the molecular environments of complexes (-)-**1** and (+)-**1** can be tuned not only in solution, but also in solid state, leading to the switching of luminescent and chiroptical properties.

Herein, we focus on the mechano-induced luminescent and chiroptical switching of complexes (-)-**1** and (+)-**1**. Two polymorphs (**Form-Y** and **Form-R**) of complex (-)-**1** have been obtained. The crystallographic studies of both forms revealed that the absorption, emission and electronic circular dichroism (ECD) spectra of these complexes at solid state were sensitive to intermolecular effects and molecular surrounding environments. The yellow forms (**Form-Y**) of complexes (-)-**1** and (+)-**1** were found to undergo color variations and crystalline-to-amorphous transformation upon mechanical grinding. These processes could be reversed by addition of a few drops dichloromethane. Both luminescence and ECD spectra exhibited significantly differences in the mechanochromic process. Moreover, we observed a more distinct luminescent switching behaviour in complexes [Pt((-)-L₁)(Dmp_i)]OTf ((-)-**2**) and [Pt((+)-L₁)(Dmp_i)]OTf ((+)-**2**) where the counteranions was OTf⁻ instead of Cl⁻. Such features are

intriguing and can be useful in novel chiroptical sensing applications.

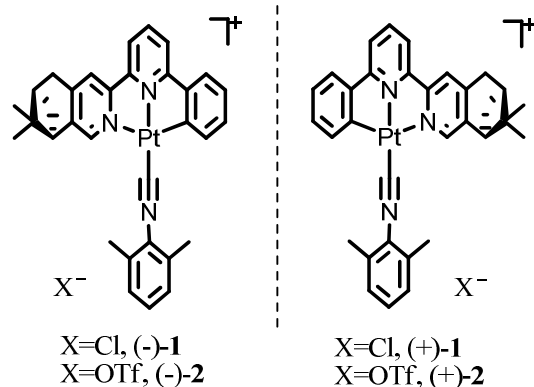


Fig. 1 Molecular structures of (-)-1, (+)-1, (-)-2 and (+)-2.

Experimental

General Methods

All reagents were purchased from commercial suppliers and used as received. Mass spectra were acquired on an LCQ Fleet ESI Mass Spectrometer. The NMR spectra were obtained on Bruker DRX-500 spectrometer. Chemical shifts are referenced to TMS. Coupling constants are given in hertz. UV-Vis spectra were measured on a UV-3600 spectrophotometer. The powder XRD patterns were recorded on a Shimadzu XD-3A X-ray diffractometer. Photoluminescence (PL) spectra were measured by Hitachi F-4600 PL spectrophotometer.

Synthesis

According to the methods reported in our previously study,¹⁰ chiral cyclometalated complexes (-)-1 and (+)-1 were conveniently prepared by the simple ligand metathesis reaction of the corresponding cyclometalated platinum(II) chloride precursor with 2,6-dimethylphenylisocyanide. Complexes (-)-2 and (+)-2 were obtained by replacement Cl⁻ with OTf⁻ anion. An aqueous solution (10 mL) of silver trifluoromethanesulfonate (0.22 mmol, 56.5 mg) was added into a 20 mL dichloromethane solution of (-)-1 (0.2 mmol, 137.4 mg). After vigorously stirring for 15 minutes, the organic phase was separated and evaporated under vacuum. Complexes (-)-2 and (+)-2 were obtained as yellow solid after evaporation.

CD spectra measurements

Solid-state ECD spectra were recorded on a Jasco J-810 spectropolarimeter. Conditions of measurements included a scanning speed of 100 nm·min⁻¹, a step size of 0.5 nm, a bandwidth of 4 nm, a response time of 1 sec, standard sensitivity setting, and an accumulation of 5 scans at room temperature. The baseline was corrected by subtracting the signal of blank sample (nujol) under the same condition. The solid-state samples were prepared by mixing the solid samples with nujol (2 mg samples mixed with 100 mg nujol) in highly dispersed state.^{9d,9e,11} Five samples were prepared and measured under the same conditions to avoid artefacts. The solid-state UV-Vis spectra were recorded with the same samples immediately after the corresponding ECD measurements.

X-ray structure determination

Single-crystal X-ray diffraction measurements were carried out on a Bruker SMART APEX CCD based on diffractometer operating at room temperature. Intensities were collected with graphite monochromatized Mo K α radiation ($\lambda = 0.71073 \text{ \AA}$) operating at 50 kV and 30 mA, using $\omega/2\theta$ scan mode. The data reduction was made with the Bruker SAINT package.¹² Absorption corrections were performed using the SADABS program.¹³ The structures were solved by direct methods and refined on F^2 by full-matrix least-squares using SHELXL-97 with anisotropic displacement parameters for all non-hydrogen atoms in all two structures. Hydrogen atoms bonded to the carbon atoms were placed in calculated positions and refined as riding mode, with C-H = 0.93 \AA (methane) or 0.96 \AA (methyl) and Uiso(H) = 1.2Ueq (C_{methane}) or Uiso(H) = 1.5Ueq (C_{methyl}). The water hydrogen atoms were located in the difference Fourier maps and refined with an O-H distance restraint [0.85(1) \AA] and Uiso(H) = 1.5 Ueq(O). All computations were carried out using the SHELXTL-97 program package.¹⁴ CCDC 1031034 and 1033960 contain the supplementary crystallographic data for this paper. These data can be obtained free of charge from The Cambridge Crystallographic Data Centre via www.ccdc.cam.ac.uk/data_request/cif.

Results and discussion

Crystal structure

Polymorphic phenomena are frequently found in square-planar platinum complexes due to the diversity in molecular arrangement achieved by varying intermolecular Pt...Pt and/or π - π interactions.⁸ The platinum(II) complexes (-)-1 and (+)-1 were prepared according to our latest studies, and their solution absorption, emission as well as chiroptical properties have been investigated.¹⁰ Notably, two polymorphisms (**Form-Y** and **Form-R**) of complex (-)-1 can be obtained by applying different recrystallizing conditions (Fig. 2). Yellow needles (**Form-Y**) of complex (-)-1 were grown slowly in acetonitrile/dichloromethane (v/v = 1:1) solution at room temperature,¹⁰ while red rods (**Form-R**) were obtained by diffusion of diethyl ether into the concentrated methanol solution at room temperature. The **Form-Y** of (-)-1 crystallizes in $P2_1$ space group of monoclinic system,¹⁰ while **Form-R** resides in $P3_121$ space group of trigonal system (Table S1, ESI[†]). The asymmetrical unit of (-)-1-**Form-Y** contains two separated molecules which are aligned parallelly in head-to-head mode, however, only one molecule is included in **Form-R** (Fig. 2). The simulated XRD patterns from single crystal structures are in good agreement with the experimental ones, manifesting the phase purity (Fig. 3).

The bond distances and bond angles in different forms of (-)-1 are almost the same (Table S2, ESI[†]) and comparable with similar Pt(C[^]N[^]N)(Dmpⁱ) derivatives reported previously.¹⁵ For both forms of (-)-1, Pt-C bond lengths range from 1.86 to 2.09 \AA , and Pt-N bond lengths are in the range 1.88-2.14 \AA . In **Form-Y**, the N1-Pt1-C2 (177.69 $^\circ$), N3-Pt2-C4 (178.13 $^\circ$) angles are close to 180 $^\circ$. However, owing to the chelate ring strain when bonding tentatively, C1-Pt1-N2 (160.09 $^\circ$) and C3-Pt2-N4 (161.24 $^\circ$) "trans angles" of the **Form-Y** deviate substantially from linearity. Similar bond angles, i.e., N1-Pt1-C2 (175.28 $^\circ$)

and C1–Pt1–N2 (162.30°) are observed in **Form-R**. The rings of 2,6-dimethylphenyl isocyanide are almost coplanar with the Pt(C[^]N[^]N) unit, with the dihedral angles between the two planes being 2.93°, 3.94° in **Form-Y**, and 3.29° in **Form-R**.

5

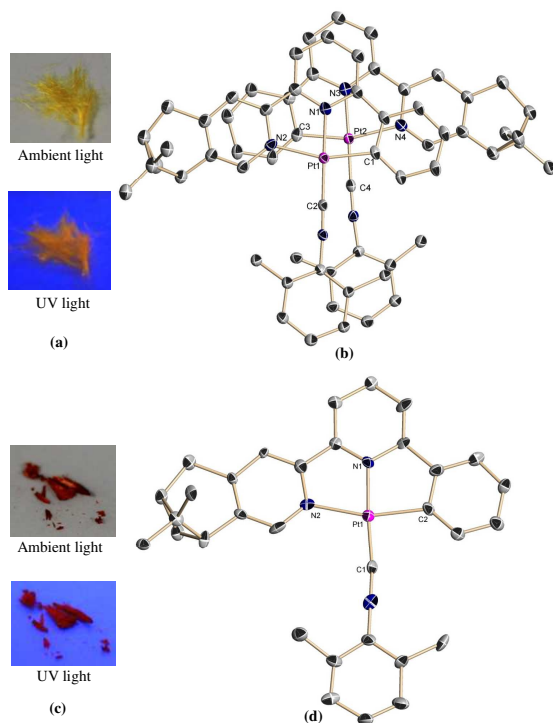


Fig. 2 (a) Photographs of polymorph (**(-)-1-Form-Y**) under ambient and ultraviolet (UV, 365 nm). (b) ORTEP plot of (**(-)-1-Form-Y**). (c) Photographs of polymorph (**(-)-1-Form-R**) under ambient and ultraviolet (UV, 365 nm). (d) ORTEP plot of (**(-)-1-Form-R**). The thermal ellipsoids are drawn at 30% probability (Hydrogen atoms, solvent molecules and anions are omitted for clarity).

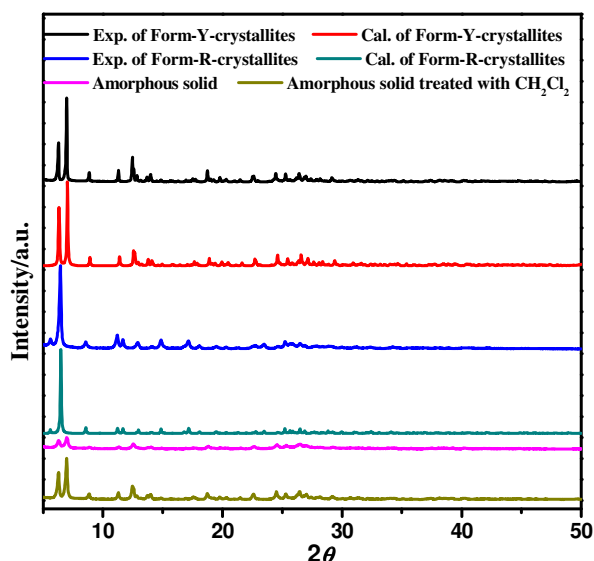


Fig. 3 Simulated and experimental XRD patterns of (**(-)-1**) with different forms (**Form-Y** and **Form-R**) as well as in the reversible mechanochromic process (Amorphous solid: crystallites of **Form-Y** after grinding for tens of seconds).

As shown in Fig. 4, the planar platinum(II) moieties of **Form-**

Y are further slip-stacked in head-to-head mode along the *a*-axis with Pt··Pt distances being 3.811 and 4.129 Å (>3.5 Å), indicating that no effective Pt··Pt interactions are involved. Although the molecules of **Form-Y** are aligned in a zig-zag style with absence of Pt··Pt interactions, distinct π - π contact (3.381 Å) of aromatic ring of 2,6-dimethylphenylisocyanide is present along the *a*-axis (Fig. S1, ESI[†]).¹⁶ Moreover, effective C–H·· π as well as C–H··H–C interactions are observed in **Form-Y** (Fig. S1, ESI[†]).¹⁷ However, the adjacent molecules in **Form-R** adopt a staggered packing mode along the *c*-axis which favours the formation of effective Pt··Pt stacking. The Pt··Pt distances are 3.397 (<3.5 Å) and 3.808 Å (Fig. 4), suggesting that substantial Pt··Pt interaction are involved.¹⁸ In addition, the dimer structures of **Form-R** are connected by C–H·· π and C–H··H–C interactions (Fig. S2, ESI[†]).¹⁷ Along the *c*-axis, one molecule of **Form-R** rotates 35.65° relative to the adjacent one (Fig. 4).

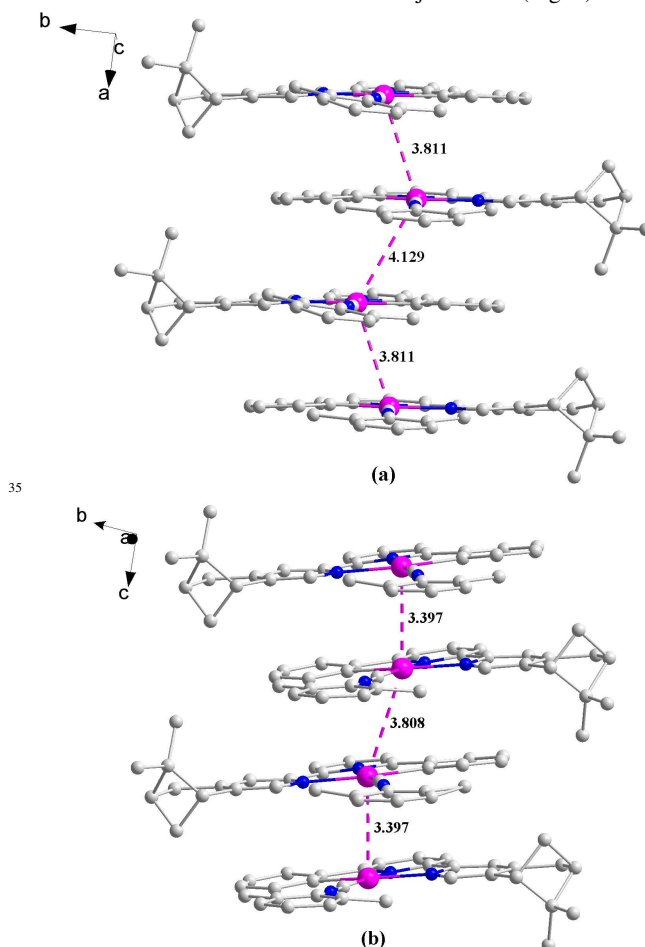


Fig. 4 (a) Crystal packing diagram of (**(-)-1-Form-Y**) depicting the Pt··Pt distances. (b) Crystal packing diagram of (**(-)-1-Form-R**) depicting the Pt··Pt distances (Hydrogen atoms, solvent molecules and anions are omitted for clarity).

Green-yellow crystals of complex (**(-)-2**) were obtained by recrystallization in acetonitrile/dichloromethane. Complex (**(-)-2**) crystallizes in *P1* space group of triclinic system (Table S1, ESI[†]). Two separated molecules are presented in the asymmetric unit (Fig. S3, ESI[†]). The plane of 2,6-dimethylphenyl isocyanide is also coplanar with the Pt(C[^]N[^]N) unit. As shown in Table S2, the relative bond lengths and angles are analogous to these in

both forms of complex (–)-1. However, the molecular arrangement of (–)-2 differs distinctly with those of (–)-1 in both forms. By applying a slipped stacking mode, the molecules of (–)-2 are aligned into one-dimensional head-to-tail chain along the *a*-axis (Fig. S4, ESI†). The Pt··Pt distances of neighboring molecules are 4.606 Å and 5.388 Å (>3.5 Å), indicating that effective intermolecular Pt··Pt interactions are non-existent in the green-yellow crystallites of complex (–)-2. The molecules in the *a*-axis are connected through Pt– π , π – π and C–H·· π interactions (Fig. S5, ESI†). The experimental XRD pattern of complex (–)-2 is examined as well, which is in line with the simulated one of single crystal structure (Fig. S6, ESI†).

Spectroscopic properties

Luminescent properties of two polymorphisms of complex (–)-1 as well as green-yellow crystals of complex (–)-2 have been investigated. The emission spectrum of crystallites of (–)-1-Form-Y is shown in Fig. 5. The crystallites of Form-Y show orange luminescence under UV radiation (Fig. 2), with a maximum wavelength at 562 nm, a shoulder peak at 529 nm, and a broad band between 600 and 800 nm. At 77 K, the emission spectrum of crystalline solids of Form-Y turns to be more structured with maximum wavelength at 540 nm (Fig. 5). The emission excited state of (–)-1-Form-Y can be designated as $^3\text{MLCT}$ mixed with $^3\text{LLCT}$.^{3b,10,15} Under UV radiation at 365 nm, the crystallites of Form-R present red luminescence (Fig. 2). The emission spectrum at room temperature displays a broad and featureless band with maximum wavelength at 646 nm (Fig. 5). It is well known that different molecular arrangements for two polymorphisms will result in different natures of frontier orbitals and excitation states, leading to dissimilar emission performances. As illustrated in the crystal packing structures (Fig. 4), distinct Pt··Pt interactions are present in Form-R. The HOMO orbital will be dominated by the metal orbital (MM), therefore the emission excited state are originated from $^3\text{MMLCT}$.¹⁵ At 77 K, the emission band of Form-R becomes narrow and the maximum wavelength is red-shifted to 658 nm. The features are characteristics for $^3\text{MMLCT}$.^{15,19} Emission spectra of (+)-1 with different solid-state forms are identical with the ones of (–)-1 (Fig. S7, ESI†).

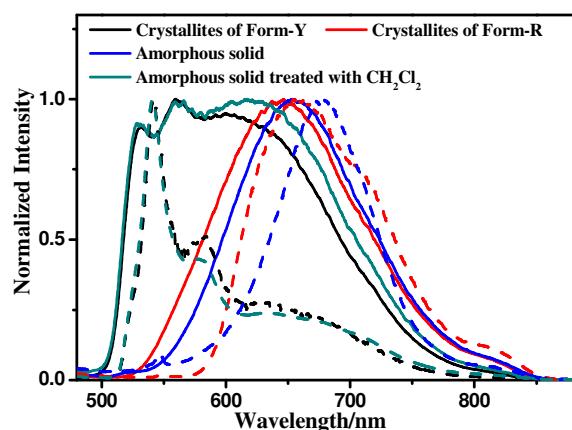


Fig. 5 Emission spectra of (–)-1 with different solid-state forms as well as in the reversible mechanochromic process at room temperature (solid line) and 77 K (dash line) (Amorphous solid: crystallites of Form-Y after grinding for tens of seconds; $\lambda_{\text{ex}} = 450$ nm).

At room temperature, crystallites of complex (–)-2 emit brightly green-yellow light under UV radiation, and a structured emission profile is observed (λ_{max} at 557 nm and a shoulder at 523 nm) (Fig. 6), which is ascribed to a mixed excited state of $^3\text{MLCT}$ and $^3\text{LLCT}$.^{3b,10,15} When the temperature was lowered from room temperature to 77 K, the emission intensity at 557 nm decreased while the one at 523 nm increased dramatically. The sideband at 523 nm evolved into a dominant emission at 77 K. Such changes are due to the different equilibrium geometries of the ground and excited state at different temperatures, which leads to different favorable vibrational modes of the electron transition and therefore different shapes of the emission spectra.²⁰ The solid emission spectrum of complex (+)-2 is identical with the one of (–)-2 (Fig. S8, ESI†).

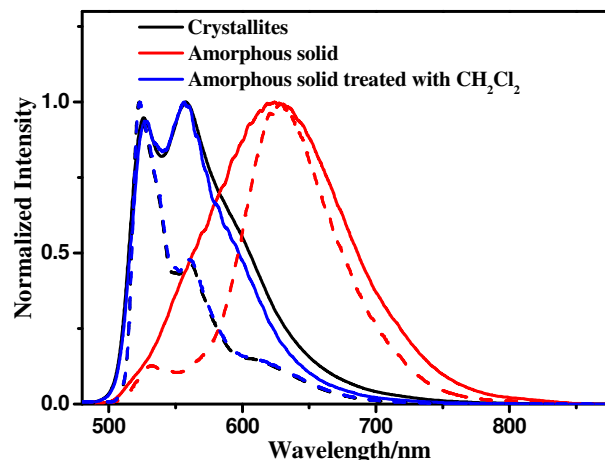


Fig. 6 Emission spectra of green-yellow crystals of (–)-2 as well as in the reversible mechanochromic process at room temperature (solid line) and 77 K (dash line) (Amorphous solid: crystallites of (–)-2 after grinding for tens of seconds; $\lambda_{\text{ex}} = 450$ nm).

Different molecular stackings and molecular surrounding environments not only induced distinct emissions but also variant chiroptical properties.²¹ In the ECD spectrum of crystallites of (–)-1-Form-Y (Fig. 7), two intense positive Cotton effects (310 and 370 nm) and three moderate negative bands (247, 273 and 415 nm) are observed. However, the solid-state ECD spectrum of (–)-1-Form-R differs distinctly with that of (–)-1-Form-Y in spite that their solid UV-Vis absorptions are similar. In the ECD spectrum of (–)-1-Form-R, two broad positive Cotton effects at 308 and 403 nm are presented. In addition, an extremely weak negative Cotton effect at 498 nm can be distinguished. For green-yellow crystallites of complex (–)-2, one intensely positive Cotton effect at 393 nm is presented, and a series of weak Cotton effects can be detected in the range of 200–350 nm (Fig. 8). To check whether any artefacts were introduced into the spectra, both solid-state forms of (+)-1 and crystallites of (+)-2 were measured under the same condition. Mirror image of ECD spectra were obtained for (+)-1 and (+)-2 (Fig. 7 and Fig. 8).

Molecular arrangements and intermolecular interactions play a significant role in the solid-state ECD. Such kind of surrounding effects have been observed before,²¹ and different intermolecular interactions (hydrogen bonds, aromatic π – π stacking, C–H·· π contact and C–H··H–C interaction) are reported to have significant influence on the ECD spectra.²² Although the isolated

molecular structures of (-)-1-Form-Y, (-)-1-Form-R as well as complex (-)-2 are similar with each other, significantly different molecular packing patterns as well as intermolecular interactions (Pt···Pt stacking, π - π contact, C-H··· π , C-H···H-C interaction) are exhibited (Fig. S1, S2 and S5, ESI[†]). The different molecular environments would induce distinct intermolecular exciton couplings (associated with projection angle and distance between dipole moments of neighboring chromophores)²³ and result in dramatically different ECD spectra. Therefore, the distinct change in solid ECD spectra should be mainly originated from the different molecular arrangements and intermolecular interactions instead of the different molecular conformations.²¹

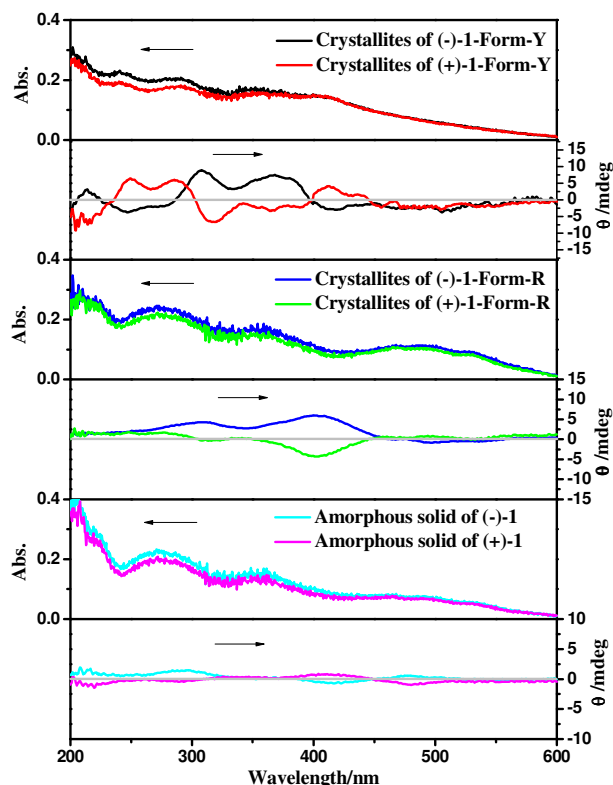


Fig. 7 Solid state UV-Vis and ECD spectra of (-)-1 and (+)-1 with different solid-state forms (Amorphous solid: crystallites of Form-Y after grinding for tens of seconds).

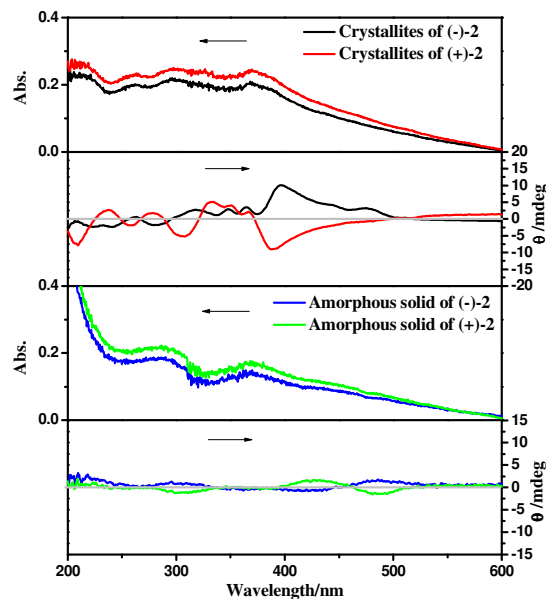


Fig. 8 Solid state UV-Vis and ECD spectra of crystallites and grinding-induced amorphous solid of (-)-2 and (+)-2.

20 Mechano-induced luminescent and chiroptical switching

Based on the polymorphisms of complex (-)-1 produced by various solvent medium, we envision that the morphological diversity may be induced by other external stimulus, leading to luminescent and chiroptical switching. Upon mechanical grinding these yellow crystallites (Form-Y) of complex (-)-1 in an agate mortar for tens of seconds, the color changes from yellow to red while the luminescence varies from orange to red under UV light (Fig. 9). In addition, the XRD pattern becomes broad and weak (Fig. 3), indicating that the crystalline solids have been transformed into almost amorphous aggregates. Upon treatment the amorphous solid powders with a few drops of dichloromethane, the orange color turns back to yellow quickly and the intense and narrow peaks are recovered in the XRD pattern (Fig. 3 and Fig. 9). The similar luminescent switching is also observed for complex (+)-1-Form-Y (Fig. S7, ESI[†]).

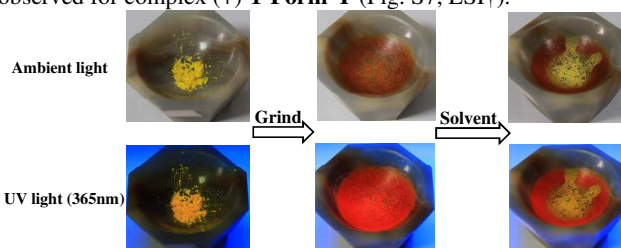


Fig. 9 Reversible mechanochromism of (-)-1. Yellow crystallites (Form-Y) of (-)-1 were ground; the yellow powders and orange emission were restored with a drop of CH_2Cl_2 . The images were obtained under ambient light and UV radiation (365 nm).

After grinding in an agate mortar, amorphous powders of (-)-1 display a broad and structureless emission band centered at 654 nm, which is similar to the emission profile of (-)-1-Form-R. With reference to previous mechanical-grinding-triggered luminescence switches about platinum(II) complexes,^{4, 6} it is assumed that the low energy emission of amorphous phase comes from ³MMLCT. For amorphous phase, the shape of the low energy emission band becomes narrow while the emission

maximum is red-shifted from 654 to 677 nm, which are also typical features of ³MMLCT excited states.^{15, 19} When a few drops of dichloromethane was added to the amorphous sample, the emission spectrum can be changed back to the same band of the original crystalline state (Fig. 5).

Moreover, the solid-state ECD spectra of crystalline solids (**Form-Y**) and amorphous powders are significantly different although their solid-state absorptions are similar. In the ECD spectrum of crystallites of (–)-**1-Form-Y**, distinct Cotton effects are distinguished. However, the amorphous phase of (–)-**1** is almost ECD silent, and only three peaks (positive: 290 and 485 nm; negative: 417 nm) with extremely weak intensity can be observed. Mirror images of solid ECD spectra were obtained for (+)-**1** in the amorphous state (Fig. 7).

Mechanical grinding not only results in square-planar platinum(II) moieties to be packed in close proximity to form a dimer or an aggregate through Pt···Pt and/or π–π contacts, but also induces the molecular arrangement changes from a well-defined ordered crystalline state to a disordered amorphous phase.^{8b, 24} Such mechanical-grinding-triggered crystalline-to-amorphous phase transition has been reported previously.²⁵ Therefore, it is proposed that, upon mechanical grinding, ordered crystalline arrangements of molecules of (–)-**1-Form-Y** have been destroyed, while the disordered aggregates with effective Pt···Pt interactions were formed in the amorphous phase, leading to a much smaller HOMO-LUMO gap and an extremely weakened chiral environment, as verified by XRD, emission and ECD spectra. Upon treating with a few drops of dichloromethane, the amorphous phase can be reverted to a well-organized crystalline state rapidly.

As exhibited in the Fig. 10, the reversible process of mechano-induced luminescence (monitored at maximum emission intensity) and ECD switching (monitored at 370 nm) of (–)-**1-Form-Y** has been repeated for multiple cycles without distinct chemical degradation.

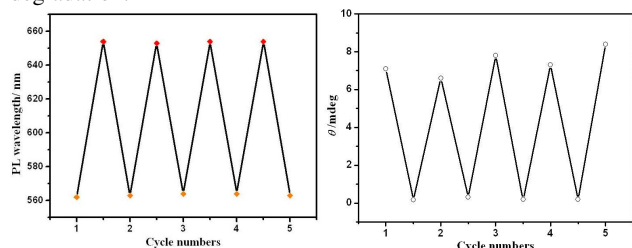


Fig. 10 Reversible process of mechano-induced luminescence (left) (monitored at maximum emission intensity) and ECD (right) (monitored at 370 nm) switching, beginning with crystallites of (–)-**1-Form-Y**.

We have also performed the mechanical grinding for **Form-R**. Similar to **Form-Y**, the crystallinity and chiroptical signals of crystallites of **Form-R** were decreased after grinding owing to crystal-to-amorphous and order-to-disorder transformation. However, a luminescent switching was not observed and the emission bands remained unchanged. This phenomenon can be rationalized by the different Pt···Pt interaction presented in the crystallites of **Form-Y** and **Form-R**. For **Form-Y**, no effective Pt···Pt interactions are involved. Mechanical grinding triggers the crystalline-to-amorphous phase transition and results in the formation of dimmers or aggregates through Pt···Pt and/or π–π contacts, the therefore lowers the emission energy. However, for

Form-R, short Pt···Pt distances have already been presented in the crystalline state. Mechanical grinding will not significantly reduce the Pt···Pt distances and lower the emission energy. Therefore, we have not observed the mechano-induced luminescent switching behavior for **Form-R**.

To gain insight into the role of counteranions in mechanochromism, the grinding experiment of green-yellow crystallites of complex (–)-**2** was further examined. When the crystallites of (–)-**2** are grinded in the mortar, the color changes from green-yellow to orange and luminescence changes from green-yellow to red (Fig. 11). Simultaneously, the crystallinity decreases dramatically owing to grind-induced crystal-to-amorphous transformation (Fig. S6, ESI†). A broad and structureless emission band ranging from 500 to 850 nm is observed at room temperature, which becomes narrow at 77 K (Fig. 6) and can be attributed to ³MMLCT excited state.^{15, 19} The maximum emission wavelength (λ_{\max} at 624 nm) of grinding powders of complex (–)-**2** is blue-shifted with relative to the grinding ones of (–)-**1-Form-Y**, owing to the bulkier counteranion OTf which blocks intermolecular interactions.^{7d, 26} The identical luminescent conversion is found for complex (+)-**2** (Fig. S8, ESI†). Similar to the mechanochromism of (–)-**1-Form-Y**, the ECD signals of complex (–)-**2** are significantly weakened after grinding (Fig. 8) due to ordered-to-disorder conversion of molecular arrangement, and only very weak positive signals at 302, 487 nm as well as a negative Cotton effect 427 can be detected. The original crystal state of (–)-**2** can be restored by treating the amorphous powders with a few drops dichloromethane, as reflected by the switches of XRD pattern and luminescence (Fig. 6 and 11; Fig. S6, ESI†).

It is noteworthy that the mechano-induced luminescent switching behavior for (–)-**2** is more distinct as compared to (–)-**1-Form-Y**. This difference can be correlated to their crystal structures. In (–)-**1-Form-Y**, molecules are packed more closely in comparison with complex (–)-**2**, as evidenced by the shorter Pt···Pt distances (3.811 and 4.129 Å for (–)-**1-Form-Y**; 4.606 and 5.388 Å for (–)-**2**) and other intermolecular contacts (Fig. 4; Fig. S1, S4 and S5, ESI†). Accordingly, the crystallites of (–)-**1-Form-Y** and (–)-**2** before grinding show significantly different emissions. Such counteranion-dependent emissions of platinum(II) complexes have been reported previously.^{4b, 7d, 7e} After grinding, the maximum emission wavelength of amorphous powders of complex (–)-**2** is blue-shifted with relative to that of (–)-**1-Form-Y** due to the weaker Pt···Pt interaction separated by bigger OTf ion. As a result, the mechano-induced luminescent switching behavior can be modulated by the counteranions.

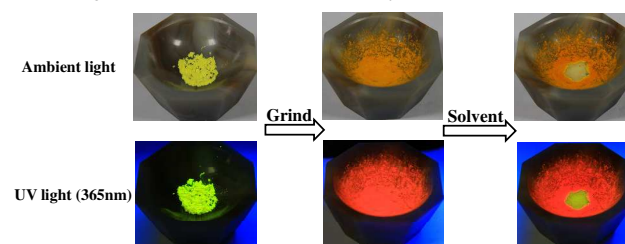


Fig. 11 Reversible mechanochromism of (–)-**2**. Green-yellow crystallites of (–)-**2** were ground; the green-yellow powders and green-yellow emission were restored with a drop of CH₂Cl₂. The images were obtained under ambient light and UV radiation (365 nm).

Conclusions

A couple of cationic cyclometalated platinum(II) complexes containing pinene functionalized chiral C^NN ligands have been prepared. Two polymorphs (**Form-Y** and **Form-R**) of (**-**)-**1** with distinct packing modes were isolated, and both of solid forms displayed different luminescent and ECD spectra. Interestingly, the crystallites of (**-**)-**1-Form-Y** exhibited intriguing mechanochromism and mechano-induced crystal-to-amorphous transformation, accompanied by significant change in luminescent and chiroptical properties. When the counteranions Cl⁻ was replaced by bulkier trifluoromethanesulfonate (OTf), a more pronounced luminescent and chiroptical switch was obtained. These changes are attributed to formation of effective Pt...Pt stackings and disordered molecular aggregates in the amorphous solids. The mechanochromic process can be reversed repeatedly by addition a few drops of dichloromethane. Moreover, mechano-responsive as well as reversion processes are very fast (within tens of seconds). Such a mechano-sensitive chiral complex may lead to useful applications as mechano-induced emission devices and solid-state chiral sensors.

Acknowledgements

This work was supported by the National Natural Science Foundation of China (91022031, 21021062), Major State Basic Research Development Program (Grant Nos. 2013CB922100, and 2011CB808704), and Doctoral Fund of Ministry of Education of China (20120091130002).

Notes and references

State Key laboratory of Coordination Chemistry, School of Chemistry and Chemical Engineering, Collaborative Innovation Center of Advanced Microstructures, Nanjing University, Nanjing 210093, People's Republic of China Fax: +86-25-83314502.; Tel: +86-25-83592969; E-mail: chli@nju.edu.cn; youxz@nju.edu.cn.

† Electronic Supplementary Information (ESI) available: Additional characterization data. CCDC 1031034 and 1033960. For ESI and crystallographic data in CIF or other electronic format see DOI: 10.1039/b000000x/

- (a) B. L. Feringa and W. R. Browne, *Molecular Switches*, Wiley-VCH, 2001; (b) S. Saha and J. F. Stoddart, *Chem. Soc. Rev.*, 2007, **36**, 77; (c) J. Crassous, *Chem. Soc. Rev.*, 2009, **38**, 830; (d) J. W. Canary, *Chem. Soc. Rev.*, 2009, **38**, 747; (e) J. W. Canary, S. Mortezaei and J. Liang, *Coord. Chem. Rev.*, 2010, **254**, 2249. (f) Z. Dai, J. Lee and W. Zhang, *Molecules* 2012, **17**, 1247.
- (a) S. Zahn and J. W. Canary, *Science*, 2000, **288**, 1404; (b) H. Miyake, K. Yoshida, H. Sugimoto and H. Tsukube, *J. Am. Chem. Soc.*, 2004, **126**, 6524; (c) T. Muraoka, K. Kinbara and T. Aida, *Nature*, 2006, **440**, 512; (d) J. Gregoliński, P. Starynowicz, K. T. Hua, J. L. Lunkley, G. Muller and J. Lisowski, *J. Am. Chem. Soc.*, 2008, **130**, 17761; (e) D. Li, Z. Y. Wang and D. Ma, *Chem. Commun.*, 2009, 1529; (f) E. Anger, M. Rudolph, C. Shen, N. Vanthuyne, L. Toupet, C. Roussel, J. Autschbach, J. Crassous and R. Réau, *J. Am. Chem. Soc.*, 2011, **133**, 3800; (g) A. Gerus, K. Šlepokura and J. Lisowski, *Inorg. Chem.*, 2013, **52**, 12450; (h) E. Anger, M. Srebro, N. Vanthuyne, C. Roussel, L. Toupet, J. Autschbach, R. Réau and J. Crassous, *Chem. Commun.*, 2014, **50**, 2854.
- (a) S. C. F. Kui, S. S.-Y. Chui, C.-M. Che and N. Zhu, *J. Am. Chem. Soc.*, 2006, **128**, 8297; (b) W. Lu, Y. Chen, V. A. L. Roy, S. S.-Y. Chui and C.-M. Che, *Angew. Chem. Int. Ed.*, 2009, **48**, 7621.
- (a) T. J. Wadas, Q.-M. Wang, Y.-J. Kim, C. Flaschenreim, T. N. Blanton and R. Eisenberg, *J. Am. Chem. Soc.*, 2004, **126**, 16841; (b) A. Han, P. Du, Z. Sun, H. Wu, H. Jia, R. Zhang, Z. Liang, R. Cao, and R. Eisenberg, *Inorg. Chem.*, 2014, **53**, 3338.
- (a) A. Y.-Y. Tam, K. M.-C. Wong and V. W.-W. Yam, *Chem. Eur. J.*, 2009, **15**, 4775; (b) S. Y.-L. Leung and V. W.-W. Yam, *Chem. Sci.*, 2013, **4**, 4228.
- (a) J. Ni, L.-Y. Zhang, H.-M. Wen and Z.-N. Chen, *Chem. Commun.*, 2009, 3801. (b) J. Ni, X. Zhang, Y.-H. Wu, L.-Y. Zhang and Z.-N. Chen, *Chem. Eur. J.*, 2011, **17**, 1171.
- (a) V. N. Kozhevnikov, B. Donnio and D. W. Bruce, *Angew. Chem. Int. Ed.*, 2008, **47**, 6286; (b) J. R. Kumpfer, S. D. Taylor, W. B. Connick and S. J. Rowan, *J. Mater. Chem.*, 2012, **22**, 14196; (c) L.-M. Huang, G.-M. Tu, Y. Chi, W.-Y. Hung, Y.-C. Song, M.-R. Tseng, P.-T. Chou, G.-H. Lee, K.-T. Wong, S.-H. Cheng and W.-S. Tsai, *J. Mater. Chem. C*, 2013, **1**, 7582; (d) M. Krikorian, S. Liu and T. M. Swager, *J. Am. Chem. Soc.*, 2014, **136**, 2952; (e) N. Kitani, N. Kuwamura, T. Tsukuda, N. Yoshinari and T. Konno, *Chem. Commun.*, 2014, **50**, 13529.
- (a) V. W.-W. Yam, K. M.-C. Wong and N. Zhu, *J. Am. Chem. Soc.*, 2002, **124**, 6506; (b) Y. Sagara and T. Kato, *Nat. Chem.*, 2009, **1**, 605; (c) X. Zhang, B. Li, Z.-H. Chen and Z.-N. Chen, *J. Mater. Chem.*, 2012, **22**, 11427. (d) X. Zhang, Z. Chi, Y. Zhang, S. Liu and J. Xu, *J. Mater. Chem. C*, 2013, **1**, 3376; (e) O. S. Wenger, *Chem. Rev.*, 2013, **113**, 3686; (f) X.-D. Wang, O. S. Wolfbeis and R. J. Meier, *Chem. Soc. Rev.*, 2013, **42**, 7834.
- (a) N. Komiya, T. Muraoka, M. Iida, M. Miyanaga, K. Takahashi and T. Naota, *J. Am. Chem. Soc.*, 2011, **133**, 16054; (b) K. M.-C. Wong and V. W.-W. Yam, *Acc. Chem. Res.*, 2011, **44**, 424; (c) K. Liu, L. Meng, S. Mo, M. Zhang, Y. Mao, X. Cao, C. Huang and T. Yi, *J. Mater. Chem. C*, 2013, **1**, 1753; (d) X.-P. Zhang, T. Wu, J. Liu, J.-C. Zhao, C.-H. Li and X.-Z. You, *Chirality*, 2013, **25**, 384; (e) X.-P. Zhang, T. Wu, J. Liu, J.-X. Zhang, C.-H. Li and X.-Z. You, *J. Mater. Chem. C*, 2014, **2**, 184.
- X.-P. Zhang, V. Y. Chang, J. Liu, X.-L. Yang, W. Huang, Y. Li, C.-H. Li, G. Muller, and X.-Z. You, *Inorg. Chem.*, **2014**, DOI: 10.1021/ic5019136.
- (a) R. Kuroda and T. Honma, *Chirality*, 2000, **12**, 269; (b) R. Kuroda, T. Harada and Y. Shindo, *Rev. Sci. Instrum.*, 2001, **72**, 3802; (c) K. Tanaka, M. Kato and F. Toda, *Chirality*, 2001, **13**, 347; (d) T. Kawasaki, K. Suzuki, K. Hatase, M. Otsuka, H. Koshima and K. Soai, *Chem. Commun.*, 2006, 1869; (e) E. Castiglioni, P. Biscarini, S. Abbate, *Chirality*, 2009, **21**, E28.
- G. M. Sheldrick, *SADABS*, an empirical absorption correction program, Bruker Analytical X-ray Systems: Madison, WI, 1996.
- G. M. Sheldrick, *Acta Cryst.*, 2008, **A64**, 112.
- D. Andrae, U. Haeussermann, M. Dolg, H. Stoll and H. Preuss, *Theor. Chim. Acta*, 1990, **77**, 123.
- (a) S.-W. Lai, H.-W. Lam, W. Lu, K.-K. Cheung and C.-M. Che, *Organometallics*, 2002, **21**, 226; (b) M.-Y. Yuen, V. A. L. Roy, W. Lu, S. C. F. Kui, G. So M. Tong, M.-H. So, S. S.-Y. Chui, M. Muccini, J. Q. Ning, S. J. Xu and C.-M. Che, *Angew. Chem. Int. Ed.*, 2008, **47**, 9895.
- C. Janiak, *J. Chem. Soc., Dalton Trans.*, 2000, 3885.
- (a) H. Suezawa, T. Yoshida, Y. Umezawa, S. Tsuboyama and M. Nishio, *Eur. J. Inorg. Chem.*, 2002, 3158; (b) D. Danovich, S. Shaik, F. Neese, J. Echeverría, G. Aullón and S. Alvarez, *J. Chem. Theory Comput.*, 2013, **9**, 1977.
- L. J. Grove, A. G. Oliver, J. A. Krause and W. B. Connick, *Inorg. Chem.*, 2008, **47**, 1408.
- (a) V. M. Miskowski and V. H. Houlding, *Inorg. Chem.*, 1991, **30**, 4446; (b) R. Büchner, C. T. Cunningham, J. S. Field, R. J. Haines, D. R. McMillin and G. C. Summerton, *J. Chem. Soc., Dalton Trans.*, 1999, 711.
- (a) *Fundamentals of Photochemistry*, ed. K. K. Rohatzi-Mukherjee, Wiley Eastern Ltd., New Delhi, Bangalore, Bombay, 1978; (b) J. A. G. Williams, *Top. Curr. Chem.*, 2007, **281**, 205.
- (a) G. Kerti, T. Kurtán, A. Borbás, Z. B. Szabó, A. Lipták, L. Szilágyi, Z. Illyés-Tünde, A. Béneyi, S. Antus, M. Watanabe, E. Castiglioni, G. Pescitelli and P. Salvadori, *Tetrahedron*, 2008, **64**, 1676; (b) G. Bringmann, K. Maksimenka, T. Bruhn, M. Reichert, T. Harada and R. Kuroda, *Tetrahedron*, 2009, **65**, 5720; (c) G. Pescitelli, S. D. Pietro, C. Cardellicchio, M. A. M. Capozzi and L.

- D. Bari, *J. Org. Chem.*, 2010, **75**, 1143; (d) H. Hussain, I. Ahmed, B. Schulz, S. Draeger, U. Flörke, G. Pescitelli and K. Krohn, *Chirality*, 2011, **23**, 617; (e) J. Frelek, M. Górecki, M. Łaszc, A. Suszczyńska, E. Vass and W. J. Szczepek, *Chem. Commun.*, 2012, **48**, 5295; (f) N. Nishiguchi, T. Kinuta, T. Sato, Y. Nakano, H. Tokutome, N. Tajima, M. Fujiki, R. Kuroda, Y. Matsubara and Y. Imai, *Chem. Asian J.*, 2012, **7**, 360; (g) N. Nishiguchi, T. Kinuta, T. Sato, Y. Nakano, T. Harada, N. Tajima, M. Fujiki, R. Kuroda, Y. Matsubara and Y. Imai, *Cryst. Growth Des.*, 2012, **12**, 1859; (h) G. Pescitelli, D. Padula and F. Santoro, *Phys. Chem. Chem. Phys.*, 2013, **15**, 795.
- 22 (a) G. A. Hembury, V. V. Borovkov and Y. Inoue, *Chem. Rev.*, 2008, **108**, 1; (b) F. Marinelli, A. Sorrenti, V. Corvaglia, V. Leone and G. Mancini, *Chem. Eur. J.*, 2012, **18**, 14680; (c) S.-Y. Xu, B. Hu, S. E. Flower, Y.-B. Jiang, J. S. Fossey, W.-P. Deng and T. D. James, *Chem. Commun.*, 2013, **49**, 8314.
- 23 (a) N. Harada and K. Nakanishi, *Circular Dichroic Spectroscopy–Exciton Coupling in Organic Stereochemistry*, University Science Books, Mill Valley, CA, 1983; (b) S. G. Telfer, T. M. McLean and M. R. Waterland, *Dalton Trans.*, 2011, **40**, 3097.
- 24 (a) T. Abe, T. Itakura, N. Ikeda and K. Shinozaki, *Dalton Trans.*, 2009, 711; (b) J. Ni, X. Zhang, N. Qiu, Y.-H. Wu, L.-Y. Zhang, J. Zhang and Z.-N. Chen, *Inorg. Chem.*, 2011, **50**, 9090; (c) X. Zhang, J.-Y. Wang, J. Ni, L.-Y. Zhang and Z.-N. Chen, *Inorg. Chem.*, 2012, **51**, 5569.
- 25 (a) T. Tsukuda, M. Kawase, A. Dairiki, K. Matsumoto and T. Tsubomura, *Chem. Commun.*, 2010, **46**, 1905; (b) N. D. Nguyen, G. Zhang, J. Lu, A. E. Sherman and C. L. Fraser, *J. Mater. Chem.*, 2011, **21**, 8409; (c) Y. Sagara and T. Kato, *Angew. Chem. Int. Ed.*, 2011, **50**, 9128; (d) W. Z. Yuan, Y. Tan, Y. Gong, P. Lu, J. W. Y. Lam, X. Y. Shen, C. Feng, H. H.-Y. Sung, Y. Lu, I. D. Williams, J. Z. Sun, Y. Zhang and B. Z. Tang, *Adv. Mater.*, 2013, **25**, 2837; (e) K. Kawaguchi, T. Seki, T. Karatsu, A. Kitamura, H. Ito and S. Yagai, *Chem. Commun.*, 2013, **49**, 11391; (f) G.-G. Shan, H.-B. Li, H.-Z. Sun, D.-X. Zhu, H.-T. Cao and Z.-M. Su, *J. Mater. Chem. C*, 2013, **1**, 1440; (g) S. Yamane, Y. Sagara, T. Mutai, K. Araki and T. Kato, *J. Mater. Chem. C*, 2013, **1**, 2648; (h) R. R. M. C.-W. Liao, W.-L. Su and S.-S. Sun, *J. Mater. Chem. C*, 2013, **1**, 5491; (i) K. Nagura, S. Saito, H. Yusa, H. Yamawaki, H. Fujihisa, H. Sato, Y. Shimoikeda and S. Yamaguchi, *J. Am. Chem. Soc.*, 2013, **135**, 10322.
- 40 26 K. Binnemans, *Chem. Rev.*, 2005, **105**, 4148.

Graphic Abstract

Chiral cyclometalated platinum(II) complexes exhibited interesting mechano-induced luminescent and chiroptical switching properties, and the mechanochromic performance can be tuned by changing the counteranions.

